Hollow-Fiber Gas-Membrane Process for Removal of NH_3 from Solution of NH_3 and CO_2

Yingjie Qin and Joaquim M. S. Cabral
Laboratório de Engenharia Bioquímica, Centro de Engenharia Biológia e Química, Instituto Superior Técnico, 1000 Lisboa, Portugal

Shichang Wang
Chemical Engineering Research Center, Tianjin University, 300072 Tianjin, P.R. China

A hollow-fiber supported gas membrane process for the separation of NH_3 from aqueous solutions containing both NH_3 and CO_2 was investigated theoretically and experimentally. A lumen laminar flow and radial diffusion model was applied to calculate the membrane wall transfer coefficient from the data stripping a single volatile component, NH_3 or CO_2, from their individual aqueous solutions. Influence of the type of membranes and operating conditions on mass-transfer rate were discussed, especially the influence of the membrane transfer coefficient on the film mass-transfer coefficient in the lumen. Appropriate configurations of the hollow-fiber modules for stripping of a single component were analyzed to optimize mass transfer. To predict the stripping of NH_3 from a solution containing NH_3 and CO_2, a mathematical model incorporating local chemical equilibria and Nernst–Planck diffusion was developed to describe the mass transport. The models described the experimental data fairly well. The experimental results showed that the supported gas membrane process can be used to remove NH_3 effectively from aqueous media containing NH_3 and CO_2.

Introduction

Supported gas membrane (SGM) separation is a mass-transfer process through a stagnant layer of a gas present in the micropores of a hydrophobic (nonwetted) membrane. It is driven by the vapor pressure difference of volatile components between the two surfaces of the membrane. This difference can be supplied by the presence of a cool liquid, a sweep gas, an absorbing liquid, a reaction solution, or by vacuum. This process is described as membrane distillation when the driving force is a vapor pressure difference caused mainly by a temperature gradient between the two fluids separated by a porous hydrophobic membrane. Alternatively, it is described as SGM absorption/stripping when the driving force is a vapor pressure difference caused either by the concentration difference of the volatile component between the two liquids separated by a porous hydrophobic membrane, or the difference of the saturate vapor pressure of the volatile component in a solution and its partial pressure in the gaseous phase on the other side of the membrane.

Applications of SGM absorption/stripping can be found in the removal of a highly volatile or volatilizable component from a gaseous stream or a dilute aqueous solution to another aqueous solution (or to a gaseous stream when the feed is an aqueous solution), for example, O_2, NH_3, CO_2, H_2S, SO_2, N_2O, HCN, CH_3COOH, Cl_2, Br_2, I_2, ethyl acetate, and phenol (Imai et al., 1982; Zhang and Cussler, 1985a, 1985b; Yang and Cussler, 1986; Kenfield et al., 1988; Semmens et al., 1989, 1990; Qin et al., 1990), in the separation of ethanol or mixed-solvents fermentation products (Udriot et al., 1989; Gostoli and Sarti, 1990), and especially in the *in situ* removal of inhibition products from fermentors (Hecht et al., 1990; Müller and Pons, 1991).

Absorption/stripping of a gas/liquid system can also be carried out with microporous hydrophilic (or wetted) membranes (Karoor and Sirkar, 1993; Kreulen et al., 1993b), which are spontaneously wetted by the absorbing solution, the gas/liquid interface being immobilized on the gas side of the

Correspondence concerning this article should be addressed to J. M. S. Cabral.
Additional address of Y. Qin: Chemical Engineering Research Center, Tianjin University, 30072 Tianjin, P. R. China.

membrane. This mode may be useful when an extremely soluble gas undergoes absorption with instantaneous reaction and a high concentration level of reactive absorbent is used. However, it would not be advantageous to operate under wetted-mode conditions for a liquid-phase-controlled process, for example, the absorption of CO_2 and SO_2 by water (Karoor and Sirkar, 1993; Kreulen et al., 1993b).

Distinct features of the SGM process are that the flow of two fluids separated by the membrane do not influence each other, resulting in an improved operational flexibility compared to conventional contactors, such as spray towers, packed beds, venturi scrubbers, and bubble columns. Thus, no special attention has to be paid to the separation of gas phase and liquid phase; the interfacial area is known *a priori*, since the membrane surface area is known and all of the membrane surface area is available for contacting regardless of how low the individual phase flow rates are; and rarely the membranes dramatically impede the transport due to the quick diffusion through the gas-filled pores. An additional advantage of the SGM process lies in its capability of simultaneously stripping (desorption or evaporation) the volatile component from an aqueous solution and its absorption (or condensation) to another aqueous solution using a single apparatus. Hollow-fiber modules provide a faster separation than conventional contractors, as the substantial increase of the interfacial area per volume overcomes the small decrease in the mass-transfer rate due to the laminar flow through the lumen. Hollow-fiber modules also are not restricted by priming, loading, flooding, weeping, foaming, backmixing, channeling, bypassing, and/or entrainment that can compromise the performance of conventional dispersion-based contactors. The overall transfer coefficients for SGM stripping are significantly higher than those associated with conventional air stripping (Semmens et al., 1989), and the treatment of acid gases with hollow-fiber modules can take place about ten times faster than that in a conventional packed column (Zhang and Cussler, 1985a; Karoor and Sirkar, 1993; Kreulen et al., 1993a).

Mathematical models have been proposed to describe the mass-transfer rate in SGM processes. The overall resistance to the transport of volatile components can be separated into three resistances in series: two fluid film resistances on both sides of the membrane and a resistance in the stagnant gas layer within the membrane micropores. Some of them may be omitted if the gas species are sparingly soluble, highly soluble, or a rapid chemical reaction occurs in the liquid phase. The membrane transfer coefficient (or resistance) depends on the regimen of gas diffusion within the membrane micropores; and the transport of combined Knudsen diffusion and Poiseuille flow has been described (Schofield et al., 1990). Empirical correlations have been used to estimate the film coefficient (Zhang and Cussler, 1985a; Yang and Cussler, 1986). A simplified model has been utilized by most researchers to interpret the experimental data, in which plug flow is assumed and lumen mass-transfer effects are lumped into a film-type mass-transfer coefficient to describe mass-transfer to the membrane lumen wall, and thus the overall transfer coefficient being treated as constant along the hollow fiber axis (Imai et al., 1982; Zhang and Cussler, 1985a, 1985b; Yang and Cussler, 1986; Kenfield et al., 1988; Semmens et al., 1989, 1990; Qin et al., 1990; Hecht et al., 1990; Müller and Pons, 1991; Kreulen et al., 1993a). A model of radial Fick's diffusion was further suggested to describe the mass transfer under laminar flow in the lumen of hollow fibers and was solved by numerical methods, in which only the mass-transfer coefficients through the membrane and through the fluid in the shell need be considered (Yamane et al., 1981; Müller and Pons, 1991; Wang et al., 1993; Karoor and Sirkar, 1993; Kreulen et al., 1993a). Kreulen et al. (1993a) predicted the influence of fiber diameter, diffusivity in liquid, liquid viscosity, liquid velocity, gas velocity, and gas phase concentration, on mass transport. Karoor and Sirkar (1993) studied the absorption by water of pure CO_2, pure SO_2, CO_2–N_2 mixtures, and SO_2–air mixtures using a laminar flow-diffusion model for the lumen side and a Happel's free surface model for the shell side. The theoretical analysis by Wang et al. (1993) can explain more precisely the experimental data present in the earlier literature. Semmens et al. (1990), Kreulen et al. (1993a), and Karoor and Sirkar (1993) discussed the influence of chemical reactions on mass transfer in SGM process.

This article investigates both theoretically and experimentally the use of microporous hydrophobic hollow fibers for the selective removal and recovery of NH_3 from aqueous media containing NH_3 or both NH_3 and CO_2. The later work is significant for the treatment of aqueous solutions and wastewater containing both NH_3 and acidic gases like CO_2, H_2S, SO_2 (Cahn et al., 1978; Mackenzie and King, 1985; Titmas and Fluto, 1993). It is especially relevant to the treatment of wastewaters containing urea, from fertilizer manufacturing plants, after being hydrolyzed by urease to NH_3 and CO_2 (Qin and Cabral, 1994, and references cited therein). The experimental results and theoretical models in the literature previously mentioned are discussed and compared with the results obtained in the present study.

Experimental Studies

Microporous hydrophobic hollow fibers, Oxyphan PP 50/280 and Plasmaphan, from Akzo/Enka were used. Hollow-fiber modules were made by potting the desired number of fibers into an external glass shell and gluing them on both ends of the shell with an epoxy resin. The characteristics of hollow-fiber modules fabricated and used in this study are provided in Table 1.

Table 1. Characteristics of the Hollow-Fiber Modules

Module No.	Hollow Fiber	R mm	R_{out} mm	Pore Diameter μm	Porosity	Z m	Shell Dia., m	A m^2	n
1	Oxyphan, PP	0.140	0.190	≤ 0.08	0.45	0.150	0.015	0.0092	70
2	Plasmaphan	0.165	0.315	0.2	0.69	0.075	0.015	0.0031	40
3	Oxyphan, PP	0.140	0.190	≤ 0.08	0.45	0.250	0.015	0.0154	70
4	Plasmaphan	0.165	0.315	0.2	0.69	0.075	0.018	0.0078	100

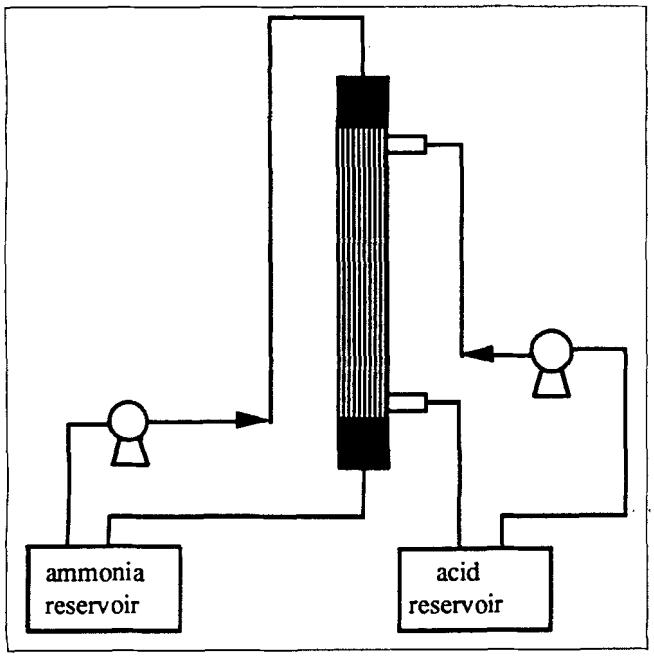

Figure 1. Experimental apparatus.

Aqueous solutions of ammonia were prepared by diluting concentrated ammonia to a given concentration. Solutions containing both NH_3 and CO_2 were made by dissolving ammonium carbamate (in an aqueous solution it will slowly revert to ammonium carbonate) or ammonium hydrogen carbonate to distilled water directly, or by mixing an NH_3 solution with an ammonium carbamate solution. The total NH_3 concentrations were determined by titration with HCl using an autotitrator/pH-controller SM Titrino 702 (Metrohm Ltd., Switzerland) with an error of less than 0.3%, and unaffected by the presence of CO_2. CO_2 solution was made by saturating distilled water with pure CO_2 gas at 1 atm, and then diluted to the desired concentration. CO_2 was titrated with NaOH using the autotitrator with errors less than 1%.

Figure 1 shows the experimental setup used for ammonia stripping/absorption studies. An aqueous solution (250 mL) with a given concentration of NH_3 (and CO_2) served as the feed. An aqueous solution (250 mL) of 2 M H_2SO_4 was used as the stripping solution. Both solutions were contained in a glass vessel with a stirring bar. Temperature was maintained by a water bath within an error of ± 0.1°C. After stirring for several minutes to attain thermal equilibrium, the feed was pumped through the module on the lumen side ($u = 0.02$–0.35 m/s), and the stripping solution ($u_s = 0.3$ m/s) through the module on the shell side. Both the feed and stripping solutions were recycled between the module and the reservoirs, respectively. Maintenance of the pH of the feed solution, when necessary, was controlled by the addition of 2 M NaOH to the feed reservoir using the autotitrator/pH-controller. Samples, 0.5 mL or 1 mL, were taken at appropriate time intervals from the feed reservoir, and the concentration of ammonia in the samples was titrated with 0.01 or 0.02 M HCl. The stripping solution was renewed when 20% of the initial concentration of H_2SO_4 was converted. In the experiment where CO_2 is stripped from an aqueous CO_2 solution, instead of the acidic stripping solution, filtered and wetted air was used as a sweep gas that was passed only once countercurrently through the shell side of the module ($u_s = 3$ m/s). In this case, a reservoir of 1 L was used and samples of 5 or 10 mL were titrated with 0.01 M NaOH.

Each experiment was repeated at least twice under the same conditions, the data reported being average values.

Theory

Mass-transfer model for stripping/absorption of a single volatile component in the fluid flowing through the lumen of hollow fibers

A conventional model was developed to describe the SGM process. The following assumptions were made to describe the fluid flow and the transport of a single volatile component in the lumen of hollow fibers and the transport across the fiber wall: (1) Fluid flow through the lumen of hollow fibers is a one-dimensional steady laminar flow, valid in most cases for hollow-fiber processes avoiding large pressure drops; (2) the laminar flow is fully developed when the mass transport through the wall of the fibers occurs at a certain distance from the entrance of the module due to the unique configuration of hollow-fiber modules where the fibers are usually epoxy bonded at the ends of the shell; (3) radial transfer of the volatile component in the lumen is by molecular diffusion, and axial diffusion is neglected because the concentration gradient in the axial direction is much smaller than that in the radial direction; (4) resistances of the membrane and of the shell fluid are unchanged with the axial direction, so the combined mass-transfer coefficient from them is treated as a constant; (5) bulk concentration of the interesting volatile component in the shell side is treated as constant in the axial direction, valid when (i) the fluid flows in excess through the shell, (ii) a pure gas is used as the feed flows through the shell, (iii) the shell is kept under vacuum, or (iv) a concentrated reactive solution flows through the shell; and (6) at the gas/liquid interface(s) Henry's law is valid for the volatile component existing in a free molecular state in the solution(s).

Therefore the concentration profiles in the lumen can be established as

$$2u\left[1-\left(\frac{r}{R}\right)^2\right]\frac{\partial C}{\partial z} = D\left[\frac{1}{r}\frac{\partial}{\partial r}\left(r\frac{\partial C}{\partial r}\right)\right] \tag{1}$$

$$B.C.1 \quad C = C_0, \quad z = 0, \quad \text{all } r \tag{2}$$

$$B.C.2 \quad \frac{\partial C}{\partial r} = 0, \quad z = 0, \quad \text{all } z \tag{3}$$

$$B.C.3 \quad D\frac{\partial C}{\partial r} = -K(C_R - C^*), \quad r = R, \quad \text{all } z \tag{4}$$

$$C_R = C^*, \quad r = R, \quad \text{all } z. \tag{5}$$

The symbols are defined in the Notation section. When the volatile component is a weak base or a weak acid like NH_3, H_2S, or CO_2, and when the stripping solution in the shell is a relatively concentrated strong acid or base solution, the absorption can be treated as an instantaneous irreversible reaction at the gas/liquid interface. Thus, C^* in Eq. 4 can be taken as zero and K can be considered as the membrane mass transfer coefficient only. Equation 5 is suitable for the

case of a pure gas flowing through the shell that is physically absorbed to the absorbent flowing through the lumen in an unwetted mode of operation (Kreulen et al., 1993; Karoor and Sirkar, 1993), which can be treated as a special example of Eq. 4 when $K = +\infty$ (Kooijman, 1973, and references cited therein). Therefore, Eqs. 1–4 can be used to describe all the cases occurring in membrane-based stripping/absorption whether the operation is in a gas/liquid or liquid/liquid system, the membrane is nonwetted or wetted (only for gas/liquid system), the fluid through the lumen of the fiber is a liquid or a gas, the gaseous phase is a pure volatile component or a gas mixture, the volatile component migrates into or out of the lumen, or the lumen concentration profile is fully established or is developing.

Suppose that

$$r' = r/R \tag{6}$$

$$C' = (C - C^*)/(C_0 - C^*) \tag{7}$$

$$z' = zD/4uR^2 = G_z^{-1} \tag{8}$$

$$Sh_w = 2KR/D, \tag{9}$$

where $G_z = 4uR^2/zD$ is the Graetz number and Sh_w is the wall Sherwood number. To be consistent with the common definition of Sherwood number, the definition of Sh_w differs by a factor of 2 from that in some literature; to make z' equal to the reciprocal of G_z, the definition of z' differs by a factor of 4 from the definition in some literature. Then Eqs. 1–4 can be reduced to the following nondimensional forms:

$$(1 - r'^2)\quad \frac{\partial C'}{\partial z'} = \frac{2}{r'}\frac{\partial}{\partial r'}\left(r'\frac{\partial C'}{\partial r'}\right) \tag{10}$$

$$z' = 0, \qquad C' = 1 \tag{11}$$

$$r' = 0, \qquad \frac{\partial C'}{\partial r'} = 0 \tag{12}$$

$$r' = 1, \qquad \frac{\partial C'}{\partial r'} = -\frac{Sh_w}{2}C'. \tag{13}$$

The preceding Fourier–Poisson equation can be solved analytically by separation of variables (Kooijman, 1973, and references cited therein). To be consistent with solving a more complicated model in the presence of CO_2, the method of orthogonal collocation was applied to obtain a numerical solution for the simulation or prediction.

As seen from Eqs. 10–13, the solution of $C'(z', r')$ is only a function of Sh_w, independent of the values of C_0 and C^*. The local cup-mixed concentration of the component at z' is defined as follows, and can be rearranged using the previously defined dimensionless variable as

$$C_z = \frac{\int_0^R 2\pi ruC\,dr}{\int_0^R 2\pi ru\,dr} = \frac{4}{R^2}\int_0^R\left[1 - \left(\frac{r}{R}\right)^2\right]rC\,dr$$

$$= 4(C_0 - C^*)\int_0^1 (1 - r'^2)r'C'\,dr' + C^*. \tag{14}$$

Thus, the dimensionless local cup-mixed concentration at z' is given by

$$C'_z = \frac{C_z - C^*}{C_0 - C^*} = 4\int_0^1 (1 - r'^2)r'C'\,dr'. \tag{15}$$

Consequently, C'_z is independent of C_0 and C^*. From Eqs. 8 and 9, it can also be concluded that, for a certain type of hollow fiber and a given gas/liquid or liquid/liquid system (i.e., K, R and D remain unchanged), C'_z will be the same for the same mean retention time, z/u. Generally, this conclusion remains true for the system in which KR/D and D/R^2 remain unchanged.

The local film coefficient in the lumen fluid k is defined by

$$N = k(C_z - C_R) = K(C_R - C^*), \tag{16}$$

then

$$k = \frac{K(C_R - C^*)}{C_z - C_R} = \frac{KC'_R}{C'_z - C'_R} \tag{17}$$

$$Sh = \frac{2Rk}{D} = \frac{2RK}{D}\frac{C'_R}{C'_z - C'_R} = Sh_w\frac{C'_R}{C'_z - C'_R} \tag{18}$$

Therefore the local lumen Sherwood number Sh at $z' = G_z^{-1}$ is independent of C_0 and C^*, but is a function of the wall Sherwood number Sh_w, which is also the conclusion of the analytical solution of Eqs. 10–13 (Kooijman, 1973).

If the fluid is recycled between the feed reservoir and the hollow fiber module and the holdup effect resulting from the pipelines can be neglected (in this study, e.g., the feed is 250 mL, while the volume of holdup liquid in the pipelines and in the lumen of the membrane is 6 mL), then

$$-V\frac{dC_0}{dt} = n\pi R^2u(C_0 - C_Z) = Q(C_0 - C_Z)$$

$$= Q(C_0 - C^*)(1 - C'_Z), \tag{19}$$

which results to

$$\ln\frac{C_0(t) - C^*}{C_0(0) - C^*} = -\frac{Q}{V}(1 - C'_Z)t, \tag{20}$$

where, Q and V are volumetric flow rates of the fluid through the lumen of the fiber module and the total volume of the fluid recycled in the lumen side, respectively, both of them being assumed to remain unchanged during the process, and C_Z is treated as the module exit concentration corresponding to the inlet concentration at the same time by pseudostate assumption.

Equation 20 implies that the logarithm of $(C_0(t) - C^*)/(C_0(0) - C^*)$ varies linearly with time, whether the lumen boundary film is developing or fully developed. This helps to explain, in mechanical terms, the hollow-fiber SGM experimental observations in the literature (Yang and Cussler, 1986; Kenfield et al., 1988; Qin et al., 1990; Hecht et al., 1990; Müller and Pons, 1991), in which simple models that

treat the overall transfer coefficient as a constant were used. In most cases, however, the lumen mass transfer coefficient is not unchanged along the fibers, unless the fibers are so long that the entrance effect can be negligible.

Stripping model of NH_3 from aqueous solution containing NH_3 and CO_2

In an aqueous solution containing both NH_3 and CO_2, the following reactions are established:

$$NH_3 + H^+ \overset{K_1}{\leftrightarrows} NH_4^+$$

$$CO_2 + H_2O \overset{K_2}{\leftrightarrows} H^+ + HCO_3^-$$

$$HCO_3^- \overset{K_3}{\leftrightarrows} H^+ + CO_3^{2-}$$

$$NH_3 + CO_2 \overset{K_4}{\leftrightarrows} NH_2COO^- + H^+$$

$$H_2O \overset{K_5}{\leftrightarrows} H^+ + OH^-.$$

The stripping of NH_3 from a solution of NH_3 and CO_2 is therefore more complicated than from a solution of NH_3. The following assumptions are made in order to describe the fluid flow and species diffusion in the lumen of the hollow fibers and their transport through the fiber wall: (1) feed flow in the lumen is steady laminar flow, and the velocity boundary layer is fully developed when mass transfer occurs; (2) reactions among all the species in the lumen feed, being much faster than the mass-transfer rate, are assumed to be at local equilibrium; (3) diffusion in the axial direction in the lumen is assumed to be negligible, the diffusion of molecules in the radial direction is given by the Fick's law, and the coupled diffusion of charged species in the radial direction is described by the Nernst–Planck equation; (4) only free NH_3 and CO_2 molecules are treated as volatile components, and the Henry's law is effective for them at the gas/liquid interfaces; (5) the stripping liquid in the shell is a nonvolatile strong acid solution, so it is preferential for the pH to be smaller than 4.5 due to the demands of posttreatment, so the concentration of ammonia in the molecular state is considered zero and the mass transfer resistance for NH_3 in the shell side does not need to be considered further (Zhang and Cussler, 1985a); (6) because the vapor pressure of ammonia is usually low, the migrating of NH_3 within the micropores may be assumed to be Knudsen's or Fick's diffusion through air (or through the mixture of CO_2 and air, when the vapor pressure of CO_2 is as high as comparable to atmospheric pressure); the migrating of CO_2 within the micropores may be assumed to be Knudsen's and/or Fick's diffusion through air, or Poiseuille flow (when its vapor pressure is high); and (7) all the physicochemical parameters of the species, such as the reaction equilibrium constants, molecular diffusion coefficients in gas or liquid, and Henry's constants, are treated as only temperature dependent; also, not being influenced by the existence of the other components, the data or the correlations can be found in the literature (Edwards et al., 1975; Geankoplis, 1983).

The continuity equation for species i in the lumen is given by the differential mass balance:

$$u_z \frac{\partial C_i}{\partial z} + \frac{1}{r}\frac{\partial}{\partial r}(rN_i) - \Sigma \nu_{ij} R_j = 0 \qquad (i = 1,8; j = 1,5), \quad (21)$$

where

$$u_z = 2u\left[1 - \left(\frac{r}{R}\right)^2\right] \quad (22)$$

and

$$N_i = -D_i \frac{\partial C_i}{\partial r} + \frac{z_i D_i C_i}{\Sigma z_l^2 D_l C_l} \Sigma z_l D_l \frac{\partial C_l}{\partial r} \quad (i = 1,8; l = 1,8). \quad (23)$$

Subscript i, $l = 1, 8$ denote species existing in the feed solution, NH_3, H^+, NH_4^+, CO_2, HCO_3^-, CO_3^{2-}, NH_2COO^-, OH^-, respectively. The other symbols are defined in the Notation section.

According to the total balance for carbon and nitrogen elements, at any point within the hollow fiber lumen solution, the net chemical reaction rate of both ammonia and carbon dioxide is zero, as from Table 2:

$$R_{NH_3,total} = (\Sigma \nu_{ij} R_j)_{NH_3} + (\Sigma \nu_{ij} R_j)_{NH_4^+} + (\Sigma \nu_{ij} R_j)_{NH_2COO^-} = 0 \quad (24)$$

$$R_{CO_2,total} = (\Sigma \nu_{ij} R_j)_{CO_2} + (\Sigma \nu_{ij} R_j)_{HCO_3^-} + (\Sigma \nu_{ij} R_j)_{CO_3^{2-}} + (\Sigma \nu_{ij} R_j)_{NH_2COO^-} = 0. \quad (25)$$

Therefore, the linear combination of the continuity equations to eliminate the rates of ionic reactions gives the following expressions:

$$\frac{\partial C_{NH_3,total}}{\partial z} = \frac{\partial C_1}{\partial z} + \frac{\partial C_3}{\partial z} + \frac{\partial C_7}{\partial z} = -\frac{1}{ru_z}\frac{\partial}{\partial r}[r(N_1 + N_3 + N_7)] \quad (26)$$

$$\frac{\partial C_{CO_2,total}}{\partial z} = \frac{\partial C_4}{\partial z} + \frac{\partial C_5}{\partial z} + \frac{\partial C_6}{\partial z} + \frac{\partial C_7}{\partial z} = -\frac{1}{ru_z}\frac{\partial}{\partial r}[r(N_4 + N_5 + N_6 + N_7)]. \quad (27)$$

Table 2. Values of Some Parameters in Eq. 28

Species	i	z_i	$\Sigma \nu_{ij} R_j$				
NH_3	1	0	$-R_1$			$-R_4$	
H^+	2	+1	$-R_1$	$+R_2$	$+R_3$	$+R_4$	$+R_5$
NH_4^+	3	+1	$+R_1$				
CO_2	4	0		$-R_2$		$-R_4$	
HCO_3^-	5	−1		$+R_2$	$-R_3$		
CO_3^{2-}	6	−2			$+R_3$		
NH_2COO^-	7	−1				$+R_4$	
OH^-	8	−1					$+R_5$

For the system under consideration, there are 10 variables ($C_{NH_{3,total}}$, $C_{CO_2,total}$, and C_i, $i=1, 8$) in these two partial differential equations; hence, the five ionic equilibrium relationships, one electroneutrality constraint, and two mass balance equations must be used to obtain the solution.

Mass balance equations:

$$C_{NH_{3,total}} = C_1 + C_3 + C_7 \tag{28}$$

$$C_{CO_{2,total}} = C_4 + C_5 + C_6 + C_7. \tag{29}$$

Electroneutrality constraint:

$$(C_2 + C_3) - (C_5 + 2C_6 + C_7 + C_8) = 0. \tag{30}$$

Chemical equilibria:

$$C_3 - K_1 C_1 C_2 = 0 \tag{31}$$

$$C_2 C_5 - K_2 C_4 = 0 \tag{32}$$

$$C_2 C_6 - K_3 C_5 = 0 \tag{33}$$

$$C_2 C_7 - K_4 C_1 C_4 = 0 \tag{34}$$

$$C_2 C_8 - K_5 = 0. \tag{35}$$

Boundary conditions:

$z = 0, \quad 0 \le r \le R$:

$$C_{NH_{3,total}} = C_{NH_3,0} \tag{36}$$

$$C_{CO_{2,total}} = C_{CO_2,0}. \tag{37}$$

$r = 0, \quad 0 \le z \le Z$:

$$\frac{\partial C_{NH_{3,total}}}{\partial r} = 0 \tag{38}$$

$$\frac{\partial C_{CO_{2,total}}}{\partial r} = 0 \tag{39}$$

$$\left(\text{as at } r = 0;\ \frac{\partial C_i}{\partial z} = 0;\ i = 1, 8\right).$$

$r = R, \quad 0 \le z \le Z$:

$$N_{NH_{3,total}} = N_{R,1} + N_{R,3} + N_{R,7} = N_{R,1} = K_{NH_3} C_1 \tag{40}$$

$$N_{CO_{2,total}} = N_{R,4} + N_{R,5} + N_{R,6} + N_{R,7} = N_{R,4} = K_{CO_2}\left(C_4 - C^*_{CO_2}\right). \tag{41}$$

Note that $N_{R,3} = N_{R,5} = N_{R,6} = N_{R,7} = 0$ according to assumption 4.

If $C_{NH_{3,total}}$ and $C_{CO_{2,total}}$ are given, the value of C_i ($i=1, 8$) can be obtained by solving Eqs. 28–35 using numerical methods. In other words, on the right side of the differential equations, Eqs. 26 and 27, C_i may be considered as functions of $C_{NH_{3,total}}$ and $C_{CO_{2,total}}$ only; therefore, the preceding differential equations, Eqs. 26 and 27, can be solved along with the boundary conditions. By using the orthogonal collocation method, these nonlinear partial differential equations are converted into a set of nonlinear ordinary differential equations, which can be solved using the Runge–Kutta method to yield the total concentration of NH_3 and CO_2 at the collocation points. Then C_i and other relevant values, for example, the mass-transfer rate, can be obtained at any point within the lumen or on the lumen surface of the hollow fiber.

When experiments were performed by recycling the feed between the reservoir and the membrane module to remove NH_3 and CO_2 separately, and the holdup effect resulting from the pipelines is neglected, the material balance can be described as follows:

$$-V\frac{dC_{NH_3,0}}{dt} = n\pi R^2 u(C_{NH_3,0} - C_{NH_3,Z}) = Q(C_{NH_3,0} - C_{NH_3,Z}) \tag{42}$$

$$-V\frac{dC_{CO_2,0}}{dt} = n\pi R^2 u(C_{CO_2,0} - C_{CO_2,Z}) = Q(C_{CO_2,0} - C_{CO_2,Z}). \tag{43}$$

These ordinary differential equations can be solved by the Runge–Kutta method.

Results and Discussion

Determination of the membrane transfer coefficient for a volatile component

In order to obtain the mass transfer coefficient through the wall of the hollow fiber, NH_3 was stripped from an aqueous solution of NH_3 in the lumen by an H_2SO_4 solution in the shell. Examples of the data obtained are presented in Figure 2. This figure shows that the logarithm of the concentration in the ammonia reservoir varies linearly with time, and is in agreement with the conclusion in the subsection on the mass transfer model (when $C^* = 0$). Comparing the simulated values with the experimental data, K can be obtained by using

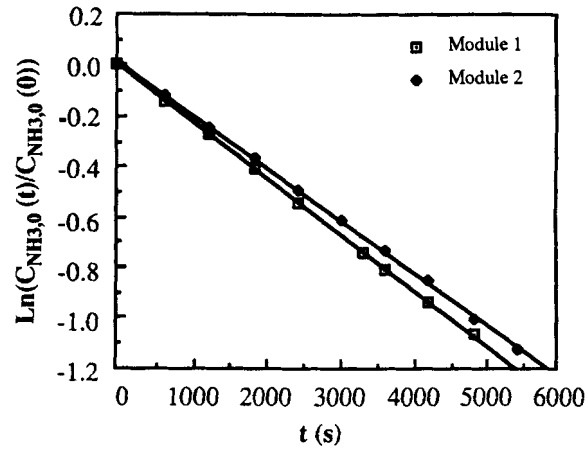

Figure 2. Typical time variation of ammonia concentration in the feed reservoir (for both modules, $T = 25°C$, $C_{NH_3,0}(0) = 0.09$ M, $u = 0.11$ m/s; the points are experimental data; the lines are corresponding best fit; the linear correlation coefficient for both lines is greater than 0.999).

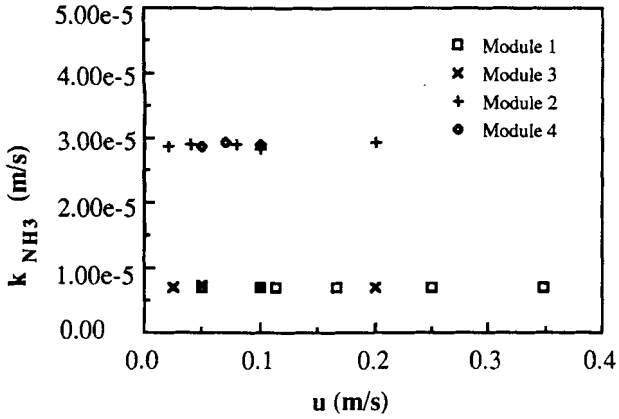

Figure 3. K vs. feed velocity through the lumen (T= 25°C; $C_{NH_3,0}$ (0) = 0.09 M; u_s = 0.1–0.3 m/s).

the least square method. The results for two kinds of fibers are shown in Figure 3. Compared with the results in an earlier paper (Wang et al., 1993), the fibers used in this work have higher mass-transfer coefficients. In spite of its thicker wall, Plasmaphan, as a result of its high porosity and large micropore diameter, has a higher K value than Oxyphan. It is evident from Figure 3 that the mass-transfer coefficient, $K = (2.90 \pm 0.04) \times 10^{-5}$ m/s for Plasmaphan and $K = (7.03 \pm 0.03) \times 10^{-6}$ m/s for Oxyphan, is almost independent of the flow rate in the lumen and in the shell, which ensures that K actually represents the characteristic of the membrane. The experiments were also carried out at various temperatures, as plotted in Figure 4, illustrating the improvement of mass transfer by increasing temperature.

Mass-transfer rate through the membrane wall can be expressed as (Yamane et al., 1981; Wang et al., 1993):

$$K = \frac{D_g \frac{\epsilon}{\tau}}{R \ln(R_{out}/R)} \frac{H}{RT}. \tag{44}$$

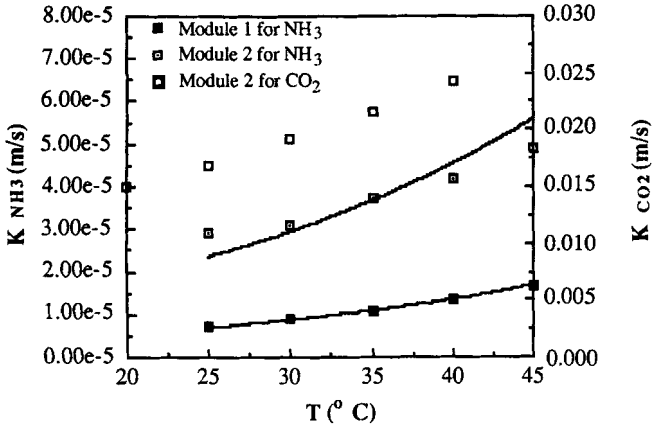

Figure 4. Membrane mass-transfer coefficient for stripping of NH_3 and CO_2 vs. temperature (the points are obtained from the experimental data; the curves are the corresponding calculated value for NH_3).

Since the ammonia concentration within the pore of the wall was small, D_g can be treated as a reciprocal average value of Fick's diffusion coefficient and Knudsen's diffusion coefficient (Geankoplis, 1983). Using the correlations of H and D_g as a function of temperature (Edwards et al., 1975; Geankoplis, 1983), the τ value from Eq. 44 can therefore be estimated to be 2.7 as the average value between 25 and 45°C for Plasmaphan and 8.0 for Oxyphan. Fixing the τ value, K is recalculated by Eq. 44 and is plotted in Figure 4. It can be seen that for the Oxyphan membrane the experimental data agree with the simulated ones; however, there is an obvious difference between the experimental and simulated values for the Plasmaphan membrane. It is difficult to find a reasonable cause for this difference.

In order to identify the mass-transfer controlling step, the local film mass-transfer coefficient in the lumen, k, obtained by solving Eqs. 1–4 to simulate the stripping of ammonia, is listed in Figure 5. It can be seen that, under experimental conditions, k is of the same order of magnitude as K for Plasmaphan; for Oxyphan, it seems that the process is controlled by membrane resistance. Both of them are mainly due to the high solubility of ammonia in water (an unusually low Henry's constant). This supports the conclusion that the membrane resistance is often significant for the reactive absorption of the gas in a strong acid or base (Zhang and Cussler, 1985a).

From Figure 5, it can be seen that k varies not only with the distance to the entrance and with the lumen liquid velocity, but also with the membrane mass-transfer coefficient K. The modeling results are redrawn in a plot of local lumen Sherwood number and logarithmic average lumen Sherwood number, as defined in the literature (Kooijman, 1972), vs. Graetz number using wall Sherwood number as a parameter, as in Figure 6. It can be seen that, after a certain distance to the entrance, Sh tends to a constant value, which means that the concentration boundary film is fully developed and the profile has constant shape over the radius. Further, it was observed that the entrance length is almost independent of Sh_w and can be calculated at about $G_z = 10$. However, Sh decreases with increasing Sh_w, even beyond the entrance region. When $Sh_w \to +\infty$ (indicated by $Sh_w = 10^{14}$), $Sh = 3.657$,

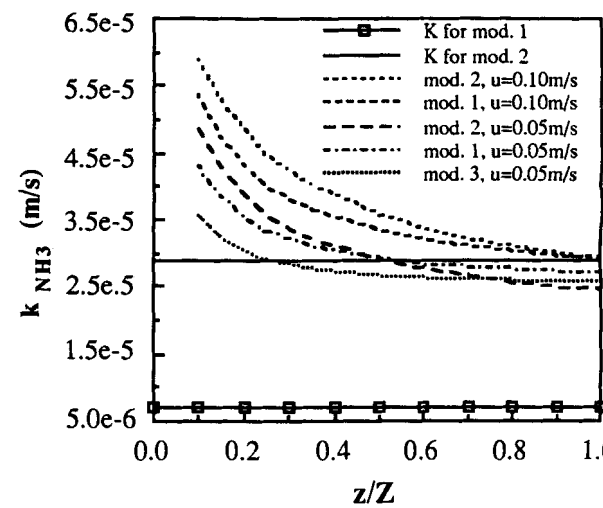

Figure 5. k vs. K for NH_3 stripping (T=25°C).

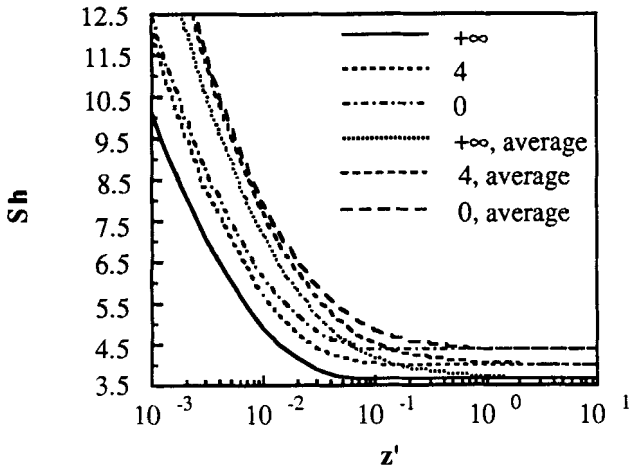

Figure 6. Simulated *Sh* and Sh_{avg} as a function of G_z with Sh_w as a parameter.

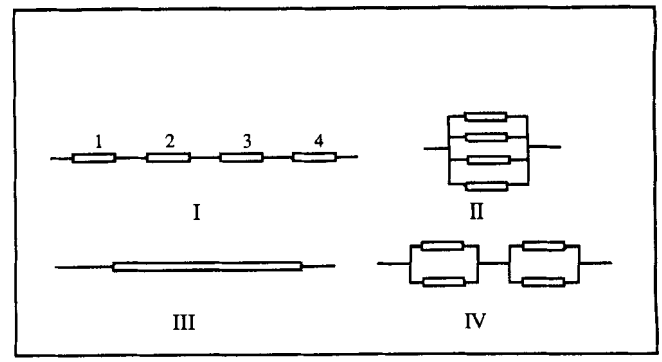

Figure 7. Potential configurations for hollow-fiber modules.

indicating that the wall resistance is negligible and the problem reduces to the classic Graetz problem of a constant concentration boundary condition; when $Sh_w \to 0$ (indicated by $Sh_w = 10^{-6}$), $Sh = 4.364$, which means that the wall resistance is dominant and the problem reduces to the case of a constant flux boundary condition at the lumen interface. This is also the conclusion of the analytical solution (Kooijman, 1972).

From Figure 6 it can also be seen that Sh_{avg} tends to a constant at about $G_z = 1$. Owing to the high diffusivity of gas molecules, for a gas flowing through the fiber lumen, the entrance length is quite short according to Eq. 8. For instance, when $R = 0.00165$ m, $D_g = 2.2 \times 10^{-5}$ m^2/s (ammonia diffusion coefficient in air at 20°C) and $u = 1$ m/s, the entrance length is only 0.005 m, which is negligible compared to the practical length of the modules. The results of Kreulen et al. (1993a) directly support this conclusion that the simulated overall mass-transfer coefficients using the membrane mass coefficient as a parameter are not a function of fiber length or gas phase velocity in the fiber lumen. For a liquid feed through the fiber lumen, the module is usually not so long that $G_z \leq 1$ (as shown in Figure 5).

In practical applications of SGM processes, the feed is usually passed only once through the module. It is not advisable to use a long module, as a higher pressure drop is required to achieve a given flow velocity. Several short modules are probably more appropriate for one treatment, and configurations of them are shown in Figure 7. Suppose that $R = 0.000165$ m, $K = 2.9 \times 10^{-5}$ m/s, $T = 25$°C, $C_{NH_3,0} = 0.1$ M, $C^* = 0$, $u = 0.10$, 0.025, 0.10 0.05 m/s for types I, II, III, and IV, respectively, $Z = 0.075$ m for types I, II and IV, and 0.3 m for III. These values of u and Z mean the total volumetric flow rate Q is the same for each type of module. For types I, II, III, and IV, the ratio of mixed-cup concentrations in the final outlet of the module to that in the inlet, C'_{total}, is calculated to be 0.557, 0.612, 0.612, and 0.586, respectively. It is noted that the stripping rate is the highest for type I *series connection*, and the lowest for type II and III, because k at every point along type I is higher than, or at least equal to, that at the same point along type III due to the entrance effect. The stripping rate for type II and type III is exactly the same due to the same mean retention time for both modules. Also, it must be noted that $C'_{total} = (C'_Z)^4$ for type I, according to the conclusion in the subsection on the mass-transfer model that C'_Z is independent of C_0. Therefore, it can be concluded that, from the point of increasing the transfer rate, the connection of modules in series is superior to the parallel one, since it makes full use of the entrance effect. However, the increase of the mass-transfer rate is obtained at the expense of a higher pressure drop. According to the Hagen–Poiseuille equation, the pressure drop through types I and III is 16-fold of type II for the same volumetric flow rate through the module. Therefore it is important, as far as economy is concerned, to strike a balance between the transfer rate and the module life.

Experiments for determining the membrane transfer coefficient for CO_2 were also performed as for NH_3. The difference is that air was used as a substitute for the acidic stripping solution. Because the wet fresh air was only single-passed rapidly through the shell of the module (CO_2 partial pressure in the air is 0.0003 atm), and the initial vapor pressure of CO_2 over the solution used was usually between 0.01 and 0.02 atm, C^* is supposed to be zero in the simulating program for the determination of K_{CO_2}. The K_{CO_2} values obtained are shown in Figure 4. It must be noted that K_{CO_2} is the combined coefficient through the membrane and the shell, and not explicitly divided between the membrane and the gas phase in the shell.

Stripping of NH_3 from an aqueous solution containing NH_3 and CO_2

Stripping of NH_3 from a solution of NH_3 and CO_2 is more difficult and more complicated when compared to the stripping from a solution of NH_3. First, the vapor pressure of NH_3 dramatically decreases due to the reduction of the pH value because of the presence of CO_2. Second, other species besides NH_3 and CO_2 exist in such a system. When the ratio of CO_2 to NH_3 in the feed solution is small, the CO_2 vapor pressure is small (e.g., at 25°C, when $C_{NH_3} = 0.1$ M, $C_{CO_2} = 0.05$ M, $P_{CO_2} = 0.002$ atm; when $C_{NH_3} = 0.1$ M, $C_{CO_2} = 0.1$ M, $P_{CO_2} = 0.106$ atm). The transport of NH_3 across the membrane wall can be taken as the diffusion of NH_3 through a stagnant air film without the influence of CO_2; hence, the membrane transfer coefficient obtained for NH_3 in the previous section can be utilized. Owing to the poor solubility of

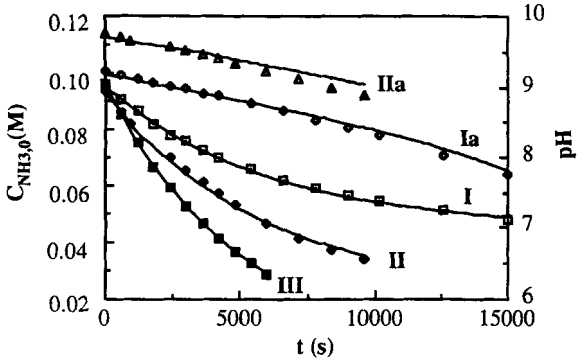

Figure 8. Typical $C_{NH_3,0}$ and pH in feed reservoir variation with time using module 1 ($T = 25°C$; $C_{NH_3,0}(0) = 0.096$ M; $u = 0.11$ m/s; curves I, II, III are predicted values of $C_{NH_3,0}$ when $C_{CO_2,0}$ was 0.048 M, 0.02 M, and 0, respectively; curve Ia, IIa predicted values of pH when $C_{CO_2,0}(0)$ was 0.048 M and 0.02 M, respectively; the points are the corresponding experimental data).

CO_2 in the acidic absorbing solution, the transport of CO_2 through the membrane wall to the reservoir of H_2SO_4 can be neglected. Comparison of the experimental data of ammonia concentration with the predicted results using the obtained K_{NH_3} are shown in Figures 8 and 9. They seem closely consistent with a maximum deviation of about 3%. The experimental and predicted values of pH are also shown in Figure 8. Neglecting the thermodynamic nonideality of the solution during the calculation may be the main reason that there exists an obvious difference at some points. In some pH ranges, the error can be attributed to the sensitivity of the pH values to the slight change in the ratio of NH_3 to CO_3 (Qin and Cabral, 1994).

The experiments were also performed at a constant pH value by adding a solution of 2-M NaOH to the feed reservoir using an autotitrator/pH controller. As seen in Figure 10, the prediction fits the experimental data fairly well: $\ln(C_{NH_3,0}(t)/C_{NH_3,0}(0)) \sim t$ is linear, which agrees with the experimental observations in the literature (Semmens et al., 1990).

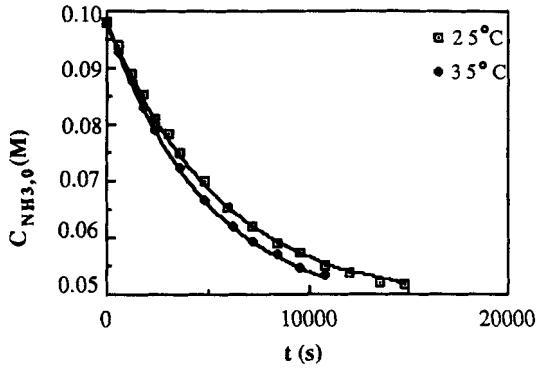

Figure 9. Typical time variation of ammonia concentration in the feed reservoir using module 2 ($u = 0.11$ m/s; $C_{NH_3,0}(0) = 0.098$ M; $C_{CO_2,0}(0) = 0.049$ M; the curves are the predicted values; the points are the corresponding experimental data).

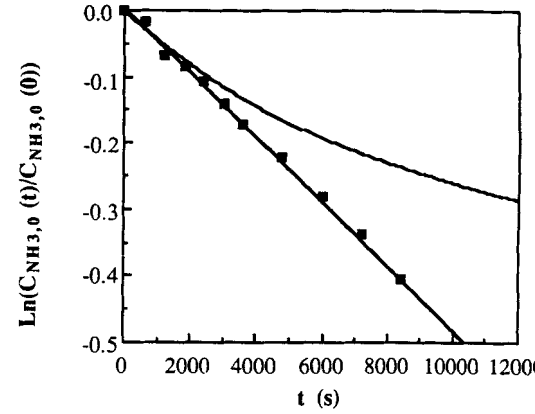

Figure 10. Time variation of ammonia concentration in the feed reservoir using module 2 ($C_{NH_3,0}(0) = 0.19$ M; pH = 8.2; $u = 0.1$ m/s; the points are the experimental data; the straight line is the predicted results; the curve shows simulated value without pH control).

It is obvious that the presence of CO_2 decreased the vapor pressure of ammonia, for example, at 25°C, $C_{NH_3} = 0.1$ M, when $C_{CO_2} = 0$, $P_{NH_3} = 1.63 \times 10^{-3}$ atm, pH = 11.1; when $C_{CO_2} = 0.05$ M, $P_{NH_3} = 7.62 \times 10^{-4}$ atm, pH = 9.18; when $C_{CO_2} = 0.1$ M, $P_{NH_3} = 5.41 \times 10^{-5}$ atm, pH = 7.77; when $C_{CO_2} = 0.2$ M, $P_{NH_3} = 2.11 \times 10^{-6}$ atm, pH = 6.35. So at a low pH value, it is almost impossible to remove NH_3 effectively by the SGM process. An improvement was obtained by first passing through a hollow-fiber module to strip NH_3 by an H_2SO_4 solution, followed by passing through another identical module, in which wet fresh air passed through the shell side, before returning to the reservoir. In the first module, the transport of CO_2 can be assumed as zero; in the second one, the transfer coefficient of CO_2 through the membrane wall can adopt the values estimated in the subsection on determination of the membrane transfer coefficient, but the transport of NH_3 through the membrane wall can be neglected due to an additional gas film resistance in the shell that does not exist in the first module. The experimental data and numerical model simulation results are presented in Figure 11. These results indicate that the addition of CO_2 stripping by sweep air dramatically increases the stripping rate of NH_3, and the theoretical predictions are consistent with the experimental data within a maximum error of 11%. The ammonia stripping rate markedly increases when compared to the rate without CO_2 stripping, although it is still low in comparison with the rate in the complete absence of CO_2. It can also be noted that an increased temperature will increase the stripping rate to a greater extent.

For a given absorbed yield, several modules in series are more practical, that is, alternating between a module to strip NH_3 using acidic solution and a module to strip CO_2 using air, continuing in this way until the desired stripping is achieved. Some simulated results are presented in Figure 12. It can be seen that, due to the high vapor pressure of CO_2, the transfer rate of CO_2 is far higher than that of NH_3, the ratio of CO_2 to NH_3 in the feed thus decreases quickly, at the same time effectively increasing the stripping rate of NH_3.

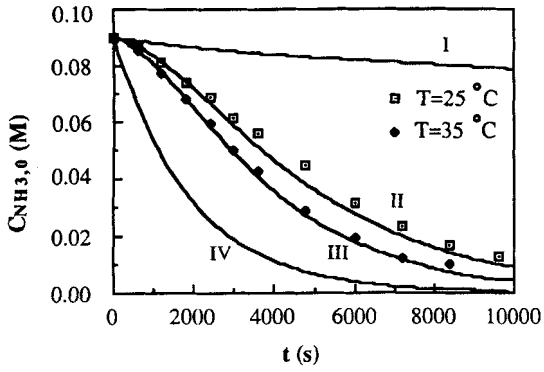

Figure 11. $C_{NH_3,0}$ vs. time by using module 4 with stripping of CO_2 following ($u = 0.1$ m/s; $C_{NH_3,0}(0) = 0.09$ M; $C_{CO_2,0}(0) = 0.09$ M; the points are the experimental data; the curves are predicted values: I. without CO_2 stripping at 25°C; II. $T = 25$°C; III. $T = 35$°C; IV. at 25°C in the absence of CO_2).

Conclusions

A hollow-fiber supported gas membrane (SGM) separation process was studied experimentally and theoretically for the stripping of single components, NH_3 or CO_2, from their individual aqueous solutions, and for the stripping of NH_3 from a solution containing both NH_3 and CO_2. The studies in the present article led to the following statements:

1. The laminar flow and radial molecular diffusion model can be used to describe the flow and mass transport of the volatile component in the lumen fluid. The model accuracy was proved by the experimental observations in the present article and in the literature.

2. From the previously mentioned model, it can be concluded that, for the volatile component,

$$C'_Z = \frac{C_Z - C^*}{C_0 - C^*}$$

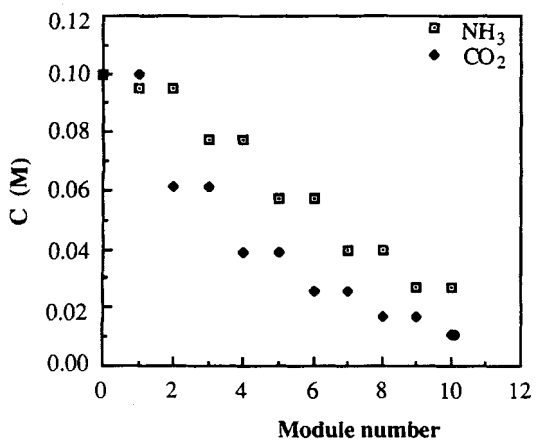

Figure 12. Simulated value of the outlet concentration of NH_3 and CO_2 varying with the number of series module 2 ($T = 35$°C; $u = 0.02$ m/s).

is a constant independent of C_0 and C^* for a given module and certain operational conditions independent of whether the lumen boundary film is developing or fully developed. Thus

$$\ln \frac{C_0(t) - C^*}{C_0(0) - C^*}$$

varies linearly with time for the batch experiments. The suggested model can satisfactorily explain the data in the literature, in which those authors explained the data by an assumption of a constant overall mass-transfer coefficient.

3. By comparing the experimental data to the model's numerical solution, we can obtain the mass-transfer coefficient K, characterizing the transport resistance of the membrane wall and the fluid in the shell. For stripping NH_3 by H_2SO_4, K is an intrinsic constant of the membrane.

4. Even if K is a constant, the lumen film coefficient k is a function of K, and k tends to a constant value at a certain distance from the entrance of the module, that is, the film boundary in the lumen is fully developed. The entrance length is a function of the Graetz number, and can be calculated at $z' = G_z^{-1} = 0.1$.

5. The entrance region effect can be negligible, that is, Sh_{avg} tends to a constant, only when $z' \geq 1$, which is satisfied for a gas phase flowing through the lumen due to the high gas diffusivity, but not, in most cases, for a liquid flowing through the lumen.

6. The membrane resistance cannot be neglected for the stripping of highly soluble components, for example, NH_3; therefore, gas membranes of smaller mass-transfer resistance are more appropriate.

7. Because of the increasing mass-transfer rate, short-length hollow-fiber modules in series are more appropriate, but at the expense of a high drop in the pressure.

8. A mathematical model incorporating lumen laminar flow, chemical equilibria, and Nernst–Planck diffusion can describe well the stripping of NH_3 from aqueous solution containing both NH_3 and CO_2 in the lumen by a strong acidic solution in the shell, using the membrane mass-transfer coefficient obtained for the single volatile component NH_3 stripping experiment.

9. When the ratio of NH_3 to CO_2 is high, the acidic stripping operation can remove NH_3 from the solution effectively with a certain decrease in the stripping rate compared to that in the absence of CO_2.

10. When the ratio of CO_2 to NH_3 is high, alternately stripping NH_3 by an acidic solution, and then CO_2 by a sweep gas, can greatly improve the removal rate of NH_3. A configuration of hollow-fiber modules in series is suggested for practical application. This is an alternative to the stripping of both NH_3 and CO_2 at an increased temperature by air, and then absorbing NH_3 in conventional contactors (Titmas and Fluto, 1993), to the removal of NH_3 by liquid membrane separation combining stream stripping (Cahn et al., 1978), to the removal of NH_3 by combined solvent extraction and steam stripping (Mackenzie and King, 1985), or to the removal of NH_3 by a supported liquid membrane process (Qin and Cabral, 1996).

Acknowledgment

The authors are grateful to Dr. P. J. Cunnah for the helpful suggestions and the stimulating discussions.

Notation

C = concentration of the volatile component in fiber lumen, M or kmol/m^3
C' = dimensionless concentration of the volatile component in fiber lumen
C_0 = inlet concentration of the volatile component at fiber entrance or the bulk concentration of the volatile component in the feed reservoir, M
$C_0(0)$ = initial concentration of the volatile component in the feed reservoir, M
$C_0(t)$ = concentration of the volatile component in the feed reservoir at time t, M
C^* = shell-side bulk concentration of a volatile component (or corresponding concentration of the volatile component in equilibrium with its bulk concentration), M
C_i = concentration of species i in lumen solution, M
C_R = concentration of the volatile component at fiber lumen surface, M
C'_R = concentration of the volatile component at lumen surface, M
C_z = mixed-cup concentration of the volatile component in fiber lumen at z, M
C'_z = local cup-mixed concentration at z
$C'_Z = C'_z$ at module outlet, especially when $C^* = 0$, the ratio of mixed-cup concentration in module outlet to inlet
C'_{total} = ratio of mixed-cup concentration in final outlet to that in the inlet
$C_{NH_3,\text{total}}$ = total concentration of ammonia in the lumen solution, M
$C_{CO_2,\text{total}}$ = total concentration of carbon dioxide in the lumen solution, M
$C_{NH_3,0}$ = total concentration of NH_3 at the lumen inlet or in the feed reservoir, M
$C_{CO_2,0}$ = total concentration of CO_2 at the lumen inlet or in the feed reservoir, M
$C_{NH_3,Z}$ = total mixed-cup concentration of ammonia at the lumen outlet, M
$C_{CO_2,Z}$ = total mixed-cup concentration of carbon dioxide at the lumen outlet, M
$C^*_{CO_2}$ = bulk concentration of carbon dioxide in the shell, M
d = fiber lumen diameter, m
D = molecular diffusion coefficient of the volatile component in lumen fluid, m^2/s
D_i = molecular diffusion coefficient of species i in lumen solution, m^2/s
D_g = gas diffusion coefficient, m^2/s
H = Henry's constant, Pa/(mol/m^3)
k_Z = film transfer coefficient in the lumen fluid at module exit, m/s
k_{avg} = average film transfer coefficient in the fiber lumen from entrance to z, m/s
K_{NH_3} = mass transfer coefficient of ammonia through the membrane wall, m/s
K_{CO_2} = overall mass transfer coefficient of carbon dioxide through the membrane wall and sweep air in the shell, m/s
K_i = equilibrium constant for reaction i
n = number of the fibers in one module
N = mass-transfer rate through the membrane wall, kmol/m^2/s
N_i = radial diffusion rate of species i in the lumen solution, kmol/m^2/s
$N_{R,i}$ = mass-transfer rate of species i through the membrane wall, kmol/m^2/s
$N_{NH_3,\text{total}}$ = total mass-transfer rate of ammonia through the membrane wall, kmol/m^3 s
$N_{CO_2,\text{total}}$ = total mass-transfer rate of carbon dioxide through the membrane wall, kmol/m^{3}s
r = radial coordinate, m
r' = dimensionless radial coordinate
R = fiber lumen radius, m
R_{out} = fiber outside radius, m
R_j = reaction rate for reaction j, kmol/m^3·s
$R_{NH_3,\text{total}}$ = net reaction rate of ammonia in the lumen solution, kmol/m^3·s
$R_{CO_2,\text{total}}$ = net reaction rate of carbon dioxide in the lumen solution, kmol/m^3·s
R = universal gas constant, J/mol·K
Sh_{avg} = average Sherwood number based on the average transfer coefficient in the lumen
T = temperature, K or °C
u = average velocity in the lumen, m/s
u_g = average gas velocity in the shell, m/s
u_s = average velocity in the shell, m/s
u_z = axial velocity at radius r, m/s
z = axial coordinate, m
z' = dimensionless axial coordinate
z_i = charge of species i
Z = effective length of the module, m

Greek letters

ϵ = porosity of the fiber wall
τ = tortuosity of the membrane wall
ν_{ij} = stoichiometric coefficient of species i in the jth reaction

Literature Cited

Cahn, R. P., N. N. Li, and R. M. Minday, "Removal of Ammonium Sulfide from Industrial Sour Water by a Liquid Membrane Process," *Env. Sci. Technol.*, **12,** 1051 (1978).
Edwards, T. J., J. Newman, and J. M. Prausnitz, "Thermodynamics of Aqueous Solutions Containing Volatile Weak Electrolytes," *AIChE J.*, **21,** 248 (1975).
Geankoplis, C. J., *Transport Processes and Unit Operations*, 2nd ed., Allyn & Bacon, Boston, p. 415 (1983).
Gostoli, C., and G. C. Sarti, "Separation of Liquid Mixtures by Membrane Distillation," *J. Memb. Sci.*, **41,** 211 (1989).
Hecht, V., L. Bischoff, and K. Gerth, "Hollow Fiber Supported Gas Membrane for *in situ* Removal of Ammonium during an Antibiotic Fermentation," *Biotechnol. Bioeng.*, **35,** 1042 (1990).
Imai, M., S. Furusaki, and T. Miyauchi, "Separation of Volatile Materials by Gas Membranes," *Ind. Eng. Chem. Process Des. Dev.*, **21,** 421 (1982).
Karoor, S., and K. K. Sirkar, "Gas Absorption Studies in Microporous Hollow Fiber Membrane Modules," *Ind. Eng. Chem. Res.*, **32,** 674 (1993).
Kenfield, C. F., R. Qin, M. J. Semmens, and E. L. Cussler, "Cyanide Recovery across Hollow Fiber Gas Membranes," *Env. Sci. Technol.*, **22,** 1151 (1988).
Kooijman, J. M., "Laminar Heat or Mass Transfer in Rectangular Channels and in Cylindrical Tubes for Fully Developed Flow: Comparison of Solutions Obtained for Various Boundary Conditions," *Chem. Eng. Sci.*, **28,** 1149 (1973).
Kreulen, H., C. A. Smolders, G. F. Versteeg, and W. P. M. Van Swaaij, "Microporous Hollow Fiber Membrane Modules as Gas-Liquid Contractors: 1. Physical Mass Transfer Process. Part 2. Mass Transfer with Chemical Reaction," *J. Memb. Sci.*, **78,** 197 (1993a).
Kreulen, H., C. A. Smolders, G. F. Versteeg, and W. P. M. Van Swaaij, "Determination of Mass Transfer Rates in Wetted and Non-Wetted Microporous Membranes," *Chem. Eng. Sci.*, **48,** 2093 (1993b).
Mackenzie, P. D., and C. J. King, "Combined Solvent Extraction and Stripping for Removal and Isolation of Ammonia from Sour Waters," *Ind. Eng. Chem. Process Des. Dev.*, **24,** 1192 (1985).
Müller, M., and M. N. Pons, "Coupling of Gas Membrane Smooth Pervaporation and Alcoholic Fermentation," *J. Chem. Tech. Biotechnol.*, **52,** 343 (1991).
Qin, R., A. K. Zander, M. J. Semmens, and E. L. Cussler, "Separating Acetic Acid from Liquids," *J. Memb. Sci.*, **50,** 51 (1990).
Qin, Y. J., and J. M. S. Cabral, "Kinetic Studies of the Urease-Catalyzed Hydrolysis of Urea in a Buffer Free System," *Appl. Biochem. Biotechnol.*, **49,** 217 (1994).
Qin, Y. J., and J. M. S. Cabral, "Hollow Fiber Supported Liquid Membrane Process for the Separation of NH_3 from Aqueous Me-

dia Containing NH_3 and CO_2," *J. Chem. Technol. Biotechnol.*, **65**, 137 (1996).
Schofield, R. W., A. G. Fane, and C. J. D. Fell, "Gas and Vapour Transport through Microporous Membranes. I. Knudsen-Poiseuille Transition," *J. Memb. Sci.*, **53**, 159 (1990).
Semmens, M. J., R. Qin, and A. Zander, "Volatile Organic Separation from Water Using Microporous Hollow Fiber Membranes," *J. Amer. Water Works Assoc.*, **81**, 162 (1989).
Semmens, M. J., D. M. Foster, and E. L. Cussler, "Ammonia Removal from Water Using Microporous Hollow Fibers," *J. Memb. Sci.*, **51**, 127 (1990).
Titmas, J. A., and P. Fluto, "Process and Apparatus for Removing Carbon Dioxide and Ammonia from Wastewater," U.S. Patent, 5,190,665 (1993).
Udriot, H., S. M. Ampuero, I. W. Marison, and U. von Stockar, "Extractive Fermentation of Ethanol Using Membrane Distillation," *Biotechnol. Lett.*, **11**, 509 (1989).
Wang, S. C., S. C. Xu, and Y. J. Qin, "Mass Transfer in Membrane Absorption-Desorption of Ammonia from Ammonia Water," *Chinese J. Chem. Eng.*, English ed., **1**, 160 (1993).
Yamane, T., M. Matsuda, and E. Sada, "Applications of Porous Teflon Tubing Methods to Automatic Fed-Batch Culture of Microorganisms: I. Mass Transfer through Porous Teflon Tubing," *Biotechnol. Bioeng.*, **23**, 2493 (1981).
Yang, M. C., and E. L. Cussler, "Designing Hollow Fiber Contactors," *AIChE J.*, **32**, 1910 (1986).
Zhang, Q., and E. L. Cussler, "Microporous Hollow Fibers for Gas Absorption: I. Mass Transfer in the Liquid; II. Mass Transfer across the Membrane," *J. Memb. Sci.*, **23**, 321 (1985a).
Zhang, Q., and E. L. Cussler, "Hollow Fiber Gas Membrane," *AIChE J.*, **31**, 1548 (1985b).

Manuscript received June 29, 1995, and revision received Nov. 3, 1995.